Journal of Molecular Graphics and Modelling 53 (2014) 118–127

Contents lists available at ScienceDirect

Journal of Molecular Graphics and Modelling

journal homepage: www.elsevier.com/locate/JMGM

An electronic environment and contact direction sensitive scoring function for predicting affinities of protein–ligand complexes in Contour®

Peter R. Lindblom, Guosheng Wu, Zhijie Liu, Kam-Chuen Jim, John J. Baldwin, Richard E. Gregg, David A. Claremon, Suresh B. Singh*

Vitae Pharmaceuticals, 502 West Office Center Drive, Fort Washington, PA 19034, United States

ARTICLE INFO

Article history:
Accepted 14 July 2014
Available online 28 July 2014

Keywords:
Scoring function
Protein–ligand interactions
Molecular orbitals
Interaction zones
Binding energy

ABSTRACT

Contour® is a computational structure-based drug design technology that grows drug-like molecules by assembling context sensitive fragments in well-defined binding pockets. The grown molecules are scored by a novel empirical scoring function developed using high-resolution crystal structures of diverse classes of protein–ligand complexes and associated experimental binding affinities. An atomic model bearing features of the valence bond and VSEPR theories embodying their molecular electronic environment has been developed for non-covalent intermolecular interactions. On the basis of atomic hybridization and polarization states, each atom is modeled by features representing electron lone pairs, p-orbitals, and polar and non-polar hydrogens. A simple formal charge model was used to differentiate between polar and non-polar atoms. The interaction energy and the desolvation contribution of the protein–ligand association energy is computed as a linear sum of pair-wise interactions and desolvation terms. The pair-wise interaction energy captures short-range positive electrostatic interactions via hydrogen bonds, electrostatic repulsion of like charges, and non-bond contacts. The desolvation energy is estimated by calculating the energy required to desolvate interaction surfaces of the protein and the ligand in the complex. The scoring function predicts binding energies of a diverse set of protein–ligand complexes used for training with a correlation coefficient of 0.61. It also performs equally well in predicting association energies of a diverse validation set of protein–ligand complexes with a correlation coefficient of 0.57, which is equivalent to or better than 12 other scoring functions tested against this set including X-Score, GOLD, and DrugScore.

1. Introduction

The ideal goal in the field of computational molecular modeling is to be able to accurately predict binding affinity of any given ligand to a protein binding site within experimental error. Both experimental and theoretical investigations have led to the identification of physically defined molecular forces responsible for the association of proteins and ligands [1,2]. The shape, electrostatics, and solvent play primary roles in the association of proteins and ligands. The complexation process is also facilitated by the favorable desolvation energy of the interfacial surfaces of the protein and the ligand. The binding forces are driven by complementary favorable interactions and opposed by repulsive forces. The evidence for the former is available through X-ray structures of protein–ligand complexes, however it is not straightforward to observe the latter experimentally. The conformational entropy of the protein and that of the ligand also contribute significantly toward free energy of binding [3,4]. There are reported treatments in the literature to capture the contribution of the conformational entropy [3–5].

The protein–ligand association processes has been simulated via free energy perturbation calculations and molecular dynamics calculations in explicit solvent [6]. However, more common application of FEP calculations has been for calculating relative binding affinities [7–9]. Even though both approaches use rigorous statistical mechanics treatment to estimate free energy of binding, they still take several days to months to calculate binding affinities, and hence are not practical for routine drug design applications.

Abbreviations: MM-GBSA, molecular mechanics/generalized born surface area; pH, polar hydrogen; nH, non-polar hydrogen; pLP, polar lone pair; nLP, non-polar lone pair.

* Corresponding author. Tel.: +1 215 461 2048; fax: +1 215 461 2006.
E-mail address: ssingh@vitaerx.com (S.B. Singh).

http://dx.doi.org/10.1016/j.jmgm.2014.07.010
1093-3263/

A more practical approach has been to use scoring functions for quick assessment of binding affinities of tens to millions of compounds in virtual screening experiments. These functions, though approximate, do empirically capture the free energy terms that contribute toward binding affinity. A large variety of empirical, force-field, and stochastic based functions have been formulated, and a significant number of these functions were developed using X-ray structures of protein–ligand complexes and experimentally determined K_d, K_i, and IC_{50} values [10–44]. The binding affinity values are reliably determined through experiment from high millimolar to picomolar range. The weaker end of the activity range is limited by the solubility of a given compound and the accuracy with which the affinity can be assessed in saturating conditions for low concentrations of protein. On the other hand, the more potent end of the activity range is limited by the ability to detect activity in a given biological assay, and the poor accuracy associated with measurements at very low concentrations of the compound and the protein.

Scoring functions differ in the way they treat the effects involved in the protein–ligand binding process. However, one thing common among the majority is that they use X-ray crystal structures of protein–ligand complexes and their associated experimental binding affinities to obtain combinations of interaction energy terms that correlate with free energy of binding. The choice of the interaction energy terms, the training set, the training methods, and validation with external data sets is critical to their applicability outside the training set. The derivation of a linear sum of interaction energy terms is a convenience, and is valid for conformations of proteins and ligands in the vicinity of near-native conformations. The prediction of ligand conformation close to the experiment can be achieved through extensive sampling, however the prediction of the protein conformation appropriate for a given ligand is still an unsolved problem.

Scoring functions trained on diverse classes of protein–ligand complexes were used to rank order molecular designs targeting a specific protein [10,11]. Scoring functions are used to make *a priori* determination whether a compound would be active or not. There are a lot of physical and chemical reasons why a compound will not exhibit activity against a given target; such as conformational flexibility, electrostatic repulsion, desolvation energy, pK_a of a charged moiety, inappropriate stereochemistry, solubility, etc. The common use of scoring functions is to rank order docked compounds [45]. Some scoring functions perform well on some classes of proteins, while some perform better on others in rank ordering docked compounds in them [45,46]. A common approach has been to use consensus among a handful of scoring functions to select compounds. In general the scoring functions were developed to handle non-covalent interactions, though some treatments include proteins with metal containing binding sites [47].

We developed an improved scoring function to assess binding affinity of compounds that get grown or assembled in the protein binding sites with Contour [48]. Contour is a structure-based design technology that grows drug-like molecules by assembling context sensitive fragments in well-defined binding pockets of proteins. The molecular assembly process in the binding site is carried out by a combinatorially efficient growth algorithm, and the selection of relevant grown molecules is assisted by a novel chemically intuitive scoring function. Contour is also capable of docking and scoring molecules in protein binding sites.

The first generation of Contour scoring function was a coarse-grained knowledge-based function trained on X-ray structures of protein–ligand complexes and associated affinity data [48]. The contact density distributions generated from interatomic interactions within 5 Å formed the basis for the scoring function. The latest generation of Contour scoring function captures the classical chemical and physical principles of interatomic interactions. An atomic model borrowing features from valence bond and VSEPR theories has been developed to represent the molecular electronic environment. The molecular orbitals of atoms are modeled by a physical construct called zones, and they represent electron lone pairs, p-orbitals, polar and non-polar hydrogens based on the atomic hybridization and polarity. A simple formal charge model was used to define polar zones (N and O atoms), and null charge for non-polar zones (carbon, halogen, and sulfur atoms). This atomic description was adopted for both the protein and the ligand atoms. The input data contained protein–ligand complexes, alternate non-native conformations of ligands as decoys, and affinity data. This input data fit using a support vector bounding algorithm generated the scoring function. A cross-validated training procedure after iterative fitting led to a linear sum of pair-wise interatomic interactions including hydrogen bonds, electrostatic repulsion, non-polar attraction, and non-polar repulsion, and a surface area based desolvation energy term.

Table 1
The zone types and their corresponding charges are given. Key, pH = polar hydrogen, nH = non-polar hydrogen, pLP = polar lone pair, nLP = non-polar lone pair, and π = represent p-orbitals. See text and Appendix for further description of the zones.

Type	Charge
pH	1
nH	0
pLP	−1
nLP	0
π	0

2. Theory and methodology

Contour employs a novel growth algorithm for efficiently searching very large chemical and conformational space for assembling drug-like molecules. Molecules are grown within a protein binding site starting from a user positioned starting fragment. Grown molecules are scored using the scoring function described below.

2.1. Contour scoring function

2.1.1. Directional contact model

Contour scoring function is based on a directional contact model in which both distance and orientation are used to characterize the geometry of atom–atom interactions. The directional model captures the basic molecular interactions such as hydrogen bond, short-range electrostatic repulsion, non-polar interaction, desolvation effect, and screening of long-range interactions by the short-range ones. The convenience of the model is that it facilitates the computation of hydrogen bonding geometry, and a novel approach to calculate surface area.

The zones representing atomic features of a given heavy atom are based on the electronic orbital hybridization state of a given atom in its molecular environment. This description of atomic representation results in the following 4 categories of zones: (1) heavy atom zone (HA) representing the direction of the bond vector to another heavy atom, and thus inaccessible for interaction; (2) polar hydrogen (pH (q+)) and non-polar hydrogen (nH (q^0)) zones; (3) polar lone pair (pLP (q−)) and non-polar lone pair (nLP (q^0)) zones,); and (4) π zones representing p-orbitals (π (q^0)); all of them schematically shown in the Appendix (Fig. 1). All polar zones arise from either a nitrogen or an oxygen atom, and depending upon the hybridization state either have a polar hydrogen zone with positive charge or a negative polar lone pair zone(s) with a negative charge. The non-polar zones from all the other heavy atoms get assigned a zero charge (Table 1). The charges for the weak interactions are

Table 2
Zone charges and the interaction table. Positive charges are assigned for polar hydrogens, and negative charges assigned to polar lone pairs (see Table 1).

Zone charge	+	–	0
+	Electrostatic repulsion	Hydrogen bond	Non-bond repulsion
–	Hydrogen bond	Electrostatic repulsion	Non-bond repulsion
0	Non-bond repulsion	Non-bond repulsion	Non-bond attraction

assigned zero values. The theory and the mathematical formulation behind zones, and their interactions are given in the Appendix.

2.1.2. Contour scoring function form

Contour scoring function was designed to capture chemical–physical features of molecular interactions via the zone-based hybrid molecular orbital representation with a simple treatment of polar and non-polar interactions. The total score for computing protein–ligand binding affinity is given by:

$$E = E_{\text{Interaction}} + E_{\text{Solvation}} \tag{1}$$

where $E_{\text{Interaction}}$ and $E_{\text{Solvation}}$ stand for pair-wise interaction and solvation scores respectively (Eq. (1)).

The first part $E_{\text{Interaction}}$ in the function is a linear combination of contributions from pair-wise zone–zone interaction types including hydrogen bonding, electrostatic repulsion, and the non-polar attraction and repulsion terms (Eq. (2)):

$$E_{\text{Interaction}} = \sum_i W_{pl}(t_i, d_i) \cdot F_i = \sum_i W_{pl}(t_i, d_i) \cdot f_{a_i} \cdot f_{b_i} = \sum_i W_{pl}(t_i, d_i) \cdot c_{a_i} \cdot Z_{a_i} \cdot c_{b_i} \cdot Z_{b_i} \tag{2}$$

where $W_{pl}(t_i, d_i)$ is a weight derived from the training set for the zone–zone interaction i with the interaction type of t_i at the distance d_i (Table 3); F_i is the interaction factor of zone–zone interaction (Eq. (7) in the Appendix). Thus for each zone–zone interaction, a geometric form factor f_i is for each zone i is obtained by multiplying the zone component, Z_i, with c_i, the cosine of the angle between the contact vector and zone vector. Thus the interaction factor F_i is a function of the angle between the zones that are in contact. For protein–ligand interactions, F_i accounts for the strength of the interaction scaled by the angle between contacting zones. For desolvation, it corresponds to the surface area that is desolvated as a result of the contact between the protein and the ligand.

Eq. (2) is applied for all types of zone–zone interactions to describe the geometry-dependent directional pair-wise interactions. For example, in the hydrogen bonding term, the interaction factor F_i is implemented to capture the hydrogen bond geometry and electronics in accordance with the orientation and interactions observed in high-resolution small molecule crystal structures [49]. Thus, the hydrogen bonding interaction term in Contour can be expressed as follows:

$$f_{ab}^{HB} = f(d_{ab}) f(\cos\theta_a) f(\cos\theta_b) \tag{3}$$

where d_{ab} is the distance between the two hydrogen bonded heavy atoms. An illustrative example is given in the Appendix.

The zone–zone charge interaction matrix is given in Table 2. The attractive interaction between the positive zone and a negative zone defines the hydrogen bond. The electrostatic repulsion represents interactions between like polar zones. The non-bond interaction is represented by the non-polar zones. The non-bond repulsion is represented by the interaction between a polar zone and a non-polar zone. The weights $W_{pl}(t_i, d_i)$ for all the interaction types were derived from the training set.

Table 3
The weights $W_{pl}(t_i, d_i)$ for protein–ligand interactions derived from the training with support vector bounding.

Interaction type	0–3.0 Å	3.0–3.5 Å	3.5–4.0 Å	4.0–5.0 Å
Hydrogen bond	0.81	0.67	0.00	0.00
Electrostatic repulsion	−1.00	−0.50	0.00	0.00
Non-bond attraction	0.00	0.00	0.00	0.00
Non-bond repulsion	0.00	0.00	0.00	0.00

The second part $E_{\text{Solvation}}$ is a contact zone based solvation term introduced to capture the electrostatic and the entropic effects of the desolvation of protein and ligand interaction surfaces involved in the complexation. It is computed by summing up the desolvation energies of all the zones at the interface of the protein and the ligand:

$$E_{\text{Solvation}} = \sum_a W_S(t_a) \cdot f_a \tag{4}$$

where $W_S(t_a)$ is a weight derived from the training set for the zone a with type t_a, f_a is a form factor $f(\cos\theta_a)$ and is related to the surface area of the atom covered by complex formation.

Steric repulsion is represented by the r^{-12} based term shown in Eq. (5), which is used to avoid strained conformations during molecular growth and is not part of the scoring function. Here r_{ij} is the distance between atoms i and j, R_i^0 and R_j^0 are the hard core van der Waals radii of atom i and j, and listed in Table 5.

$$E_{\text{Steric}} = \left(\frac{r_{ij}}{R_i^0 + R_j^0} \right)^{-12} \tag{5}$$

The Contour scoring function form and the terms that define it were derived from the training process. It consists of an empirical physical model with a sum of discrete linear energy terms derived by training on high-resolution crystal structures and experimentally determined affinity data. The scoring function was designed to capture essential features of molecular interactions via the zone-based representation with a simple treatment of polar and non-polar interactions.

2.2. Input data

A compilation of 203 protein–ligand complex X-ray structures spanning 10 families of proteins (Chart 1) were collected historically with relevance to the internal drug discovery programs used as training set for the scoring function. A systematic analysis was conducted to make sure that all types of interactions and solvation terms are statistically significant in the training set. We included complexes that contain drug-like molecules. This input data set did not include metalloenzymes, multiply charged ligands, and fatty acids. The list of PDB codes and the associated activity data are given in the excel spread sheet included as supplementary material (S1). The activity data for most of the complexes were compiled from the literature, a few renin inhibitor complexes from Vitae, and the rest from PBDbind data set [50].

The protein–ligand complexes were separated into protein chains and ligands. All waters, cosolvents, and other extraneous ligands without measured binding data were omitted in modeling protein–ligand interactions. In each case all protein chains were modeled using Maestro's protein preparation wizard [51] to add hydrogen atoms, optimize the sidechain orientations, hydrogen bond interactions, and protonation states. The protonation states and the sidechain conformations resulting from Maestro were directly used without further modification. Ligands were

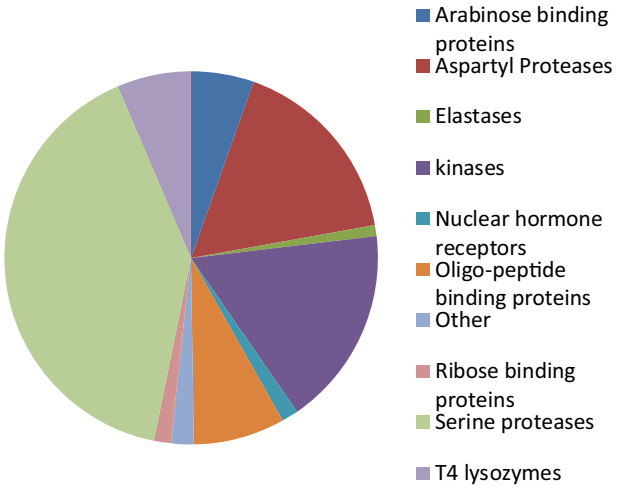

Chart 1. Distribution of protein families from protein–ligand complexes used in the training set.

processed with Maestro tool Assign-bond-orders [52]. The bond orders and protonation states were visually checked, and the protonation states of positively charged species were determined by the bond orders and the expected pKa of the atom at pH 7. For each ligand at least 25 distinct conformations were generated with Contour growth algorithm. In the training process the X-ray conformation served as the best scoring conformer, while the computed conformations were treated as non-native or decoys and constrained to score less than the X-ray conformer.

2.3. Support vector bounding

An algorithm designed to take input data with activity values, discrete bounds, and classification criteria was used to generate the Contour scoring function. This methodology is a hybrid of support vector machine and support vector regression methods, in which classification and regression modeling techniques are combined. The algorithm shares several advantages of both these techniques, such as a sparse solution space, absence of local minima, the ability to control the capacity of the system to prevent overfitting, and the ability to model non-linear functions using linear operations in a kernel-induced feature space [53]. Through fitting the scoring function with the training set, the algorithm will generate the weights for zone–zone interaction and zone solvation descriptors, but it also will provide the *z*-scores representing the significance of the descriptors to the models. The *z*-scores are determined from multi-fold cross validations using equation 6:

$$z(i) = \frac{\mu(i)}{\sigma(i)} \quad (6)$$

where $\mu(i)$ is the mean of computed weights for descriptor i from multi-fold cross validations and $\sigma(i)$ is the standard deviation.

3. Results

3.1. Scoring function model generation

The zones used for protein–ligand interactions are as follows: polar hydrogen (pH), non-polar hydrogen (nH), polar lone pair (pLP), non-polar lone pair (nLP), and π (p-orbitals). These zones thus allow four major types of protein–ligand interactions: the hydrogen bond, electrostatic repulsion, non-bond interaction, and non-bond repulsion (Tables 1–2). Accordingly zone desovlation

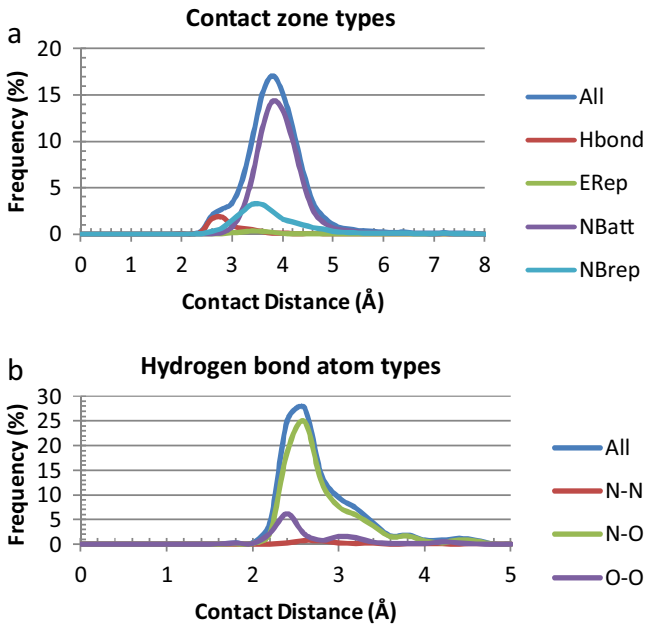

Chart 2. Histogram plots of zone–zone interactions from the protein–ligand X-ray training set generated using the Contour's atomic contact model and 8 Å cutoff: (a) distribution of all zone–zone interactions and (b) distribution of hydrogen bond interaction types.

effects are represented by protein polar zone, protein non-polar zone, ligand polar zone, and ligand non-polar zone.

3.2. Distance-dependent distribution of zone–zone interactions

In order to visualize the distribution of zone–zone interaction distances in the input X-ray structures of protein–ligand complexes in the training set we computed the interaction distances using an 8 Å cut-off and our contact model (Chart 2). It is interesting to note, not unexpectedly, that all the zone–zone contacts from the density plot are in the range of 2.4–5.0 Å (Chart 2a). The non-bond interactions including non-bond attraction and non-bond repulsion display a normal distribution within 5.0 Å. Also worth noting is that the occurrence of electrostatic repulsion in the X-ray structures is rare. This is consistent with the idea that protein–ligand association is mainly driven by attractive forces with minimal or no repulsive forces. As expected the hydrogen bond interactions largely fall within a narrow range of 2.4–3.5 Å with the highest peak observed at 2.8 Å (Chart 2b). On the basis of this distribution 4 distance bins were proposed: 0–3.0 Å, 3.0–3.5 Å, 3.5–4.0 Å, and 4.0–5.0 Å. Thus, a total of 20 descriptors were used in deriving the final scoring function that include 16 zone–zone interactions arising from 4 types of interactions for 4 distance bins, and 4 desolvation terms.

3.3. Training of Contour scoring function

The support-vector bounding algorithm was applied to all 20 descriptors computed from the 203 X-ray structures of protein–ligand complexes and their decoys to derive descriptor weights by simultaneously fitting to the associated binding constants. The iterative process of fitting a random set of 80% of the input data set followed by the prediction of the binding affinity for the rest of the 20% of the data set was continued until the weights achieved convergence. The descriptors that exhibited significant contributions to the prediction of binding affinity of protein–ligand complexes were identified using *z*-score, which led to the selection of terms with non-zero weights including 2

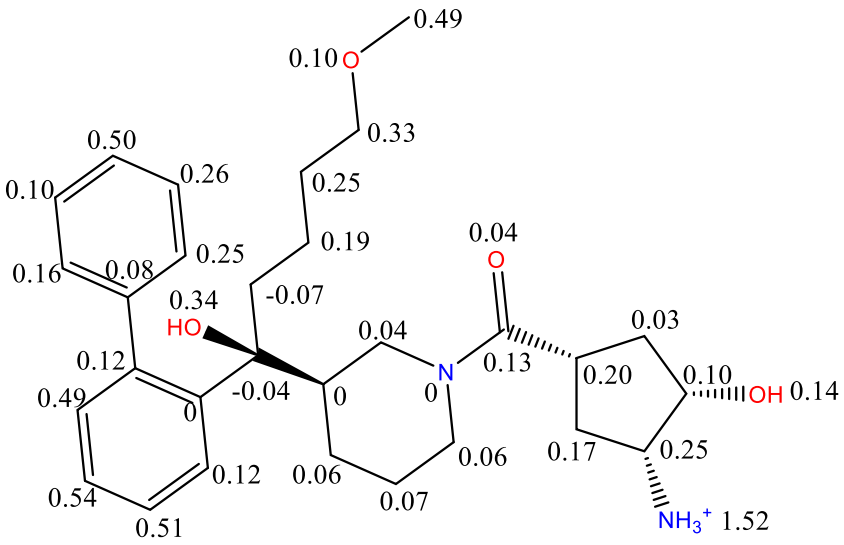

Fig. 1. Contour scores for renin inhibitor from the X-ray structure (PDB code 3Q3T). The pK_i of the compound is 7.44 and the predicted Contour score is 7.52. For each atom, the Contour score is summed up to show their binding contribution.

Table 4
The weights $W_S(t_i)$ solvation derived from training. The negative weights represent penalty for desolvating polar zones, and positive weights represent benefit in desolvating non-polar zones.

Interaction type	Non-polar desolvation	Polar desolvation
Ligand zones	0.08	−0.14
Protein zones	0.08	−0.14

hydrogen bond and 2 electrostatic repulsion terms (≤3 Å, 3.0–3.5 Å) for the protein–ligand interactions, and 4 non-polar and polar desolvation terms for ligand and protein zones. Thus there were a total of 8 parameters or descriptors used as input for training the final scoring function with the entire training set. The final zone–zone interaction descriptors, and their associated weights are shown in Table 3, and the weights associated with the zone desolvation terms are shown in Table 4. The final Contour score is approximately equivalent to pK_i ($-\log K_i$). For example, scores of 6.0, 7.0, 8.0, 9.0, and 10.0 correspond to binding constants of 1000, 100, 10, 1.0, and 0.1 nM respectively. Fig. 1 illustrates the calculated Contour scores for a renin compound VTP-000026080, where the $-\log K_i$ (expt.) is 7.44 and the computed score is 7.52. The contribution from hydrogen bonding is 3.88, and that from desolvation is 3.65 for the computed score.

The predictive performance of the final model of the scoring function for the 203 protein–ligand complexes in the training set is shown in Charts 3 and 4. The model shows a correlation of 0.61

Table 5
Hard core van der Waals radii used in steric function adopted from Amber 4.0 force field [63].

Element	Radius
H	1.0
C	1.6
N	1.5
O	1.4
P	1.9
S	1.85
F	1.4
Cl	1.8
Br	1.85
I	2.1
B	1.6
Metal ions	1.7

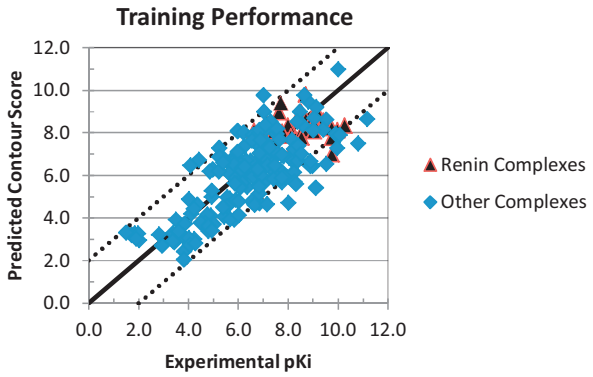

Chart 3. Performance of the Contour scoring function on the training set, where pK_i is defined as $-\log(K_i)$. The Contour score is expressed as $-\log(K_i)$ predicted. The correlation of the above prediction is 0.61, and RMSE of 1.20. The solid line runs through the origin for reference, and the dashed lines above and below mark the 2.0 log units from this reference line.

indicating an acceptable level of accuracy of the estimation of binding affinities. A clear separation of the weak binders (>1000 mM) from the strong ones (<1 μM) leads the scores to be reliable in identifying grown molecules that are most likely to exhibit activity. Thus, Contour scoring function serves the purpose of identifying compounds that are worth pursuing.

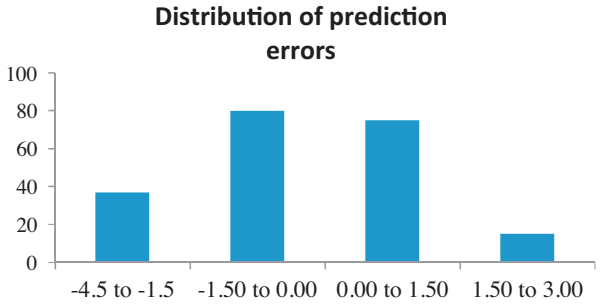

Chart 4. Distribution of differences in predicted versus experimental values. The negative values indicate that the scoring function is underpredicting the activity, and the positive values conversely indicate overprediction. The scoring function predicts equal to or less than the experimental value in 56% of the cases, however 75% of the predictions are within 1.5 log of the observed values.

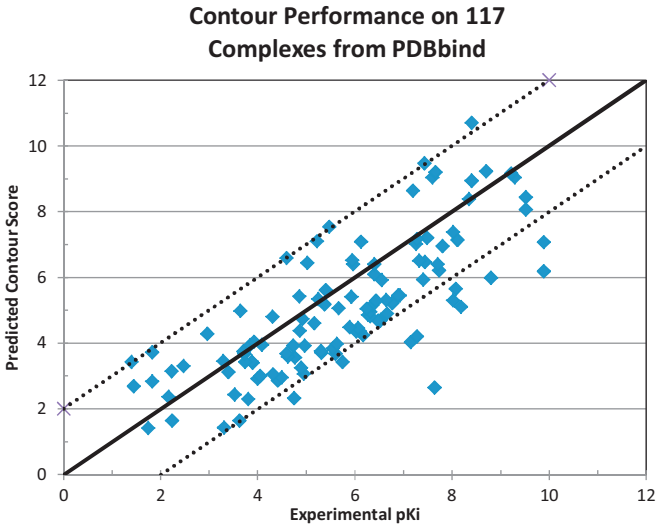

Chart 5. Contour scoring function performance on a validation set of 117 protein–ligand complexes [35]. The solid line and the dashed lines as defined in Chart 3. Contour score is meant to be equivalent to pK_i. A correlation of 0.57 is observed with this data set and an RMSE of 1.61.

3.4. Scoring function validation: external validation set of protein–ligand complexes

A physically meaningful and reasonably accurate scoring function developed with a careful choice of molecular descriptors, and a training process identified interaction energy terms that have tangible relationship to the association process of proteins and ligands. This was further buttressed by a solid performance of the scoring function with a good correlation between the theory and the experiment. A scoring function thus derived boosted our confidence to test its predictive power on protein–ligand complexes not in the training set. The performance of the scoring function was tested on a diverse set of protein–ligand complexes.

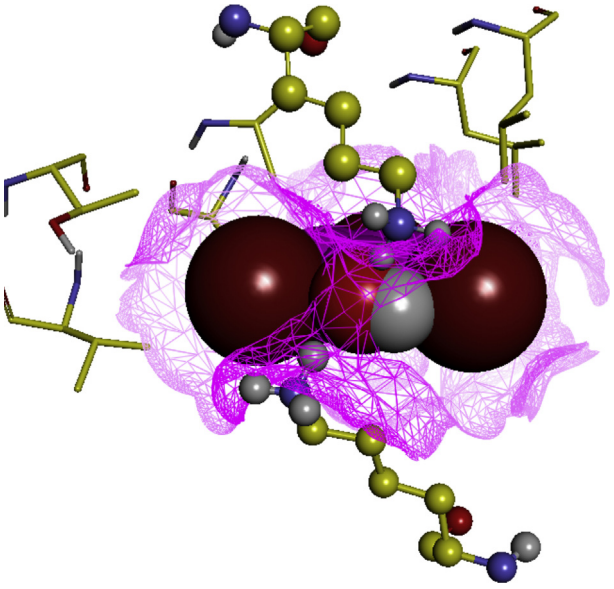

Fig. 2. Crystal structure of human transthyretin complexed with bromophenol (PDB code 1e5a), an outlier in Chart 5. Contour predicted an activity of 2.7 versus 7.6 observed for the bromophenol shown in the structure. This example appears to be an outlier for most of the scoring functions tested by Cheng et al. [35]. Two monomer units of the protein bound to bromophenol with lysines from each monomer interacting with the hydroxyl of bromophenol. The non-polar residues shown for the monomer on the top are symmetrically opposite to the ones from the second monomer on the bottom. The picture was rendered using Accelrys' Discovery Studio 3.5 [62].

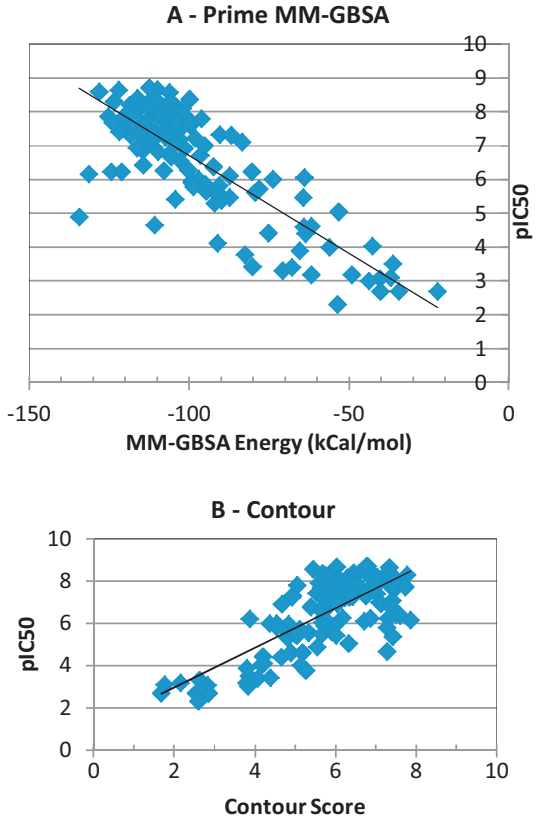

Chart 6. Correlation plots for 128 X-ray structures of non-peptidic BACE1 inhibitors. In panel A, the calculated interaction energies with MM-GBSA plotted against IC50 values. The energies with MM-GBSA were calculated using the protein from pdb code 2OHU [61] and X-ray bound conformations of ligands. The strain energy correction was not used. The MM-GBSA energies were computed with Prime program in Maestro interface from Schrodinger Inc. [52]. A correlation of 0.66 and root mean squared error (RMSE) of 0.97 was obtained with the Prime MM-GBSA protocol. In Panel B, Contour scores plotted against the IC50 values, with a correlation of 0.55 and an RMSE of 1.11.

Contour's performance on this validation set with a correlation of 0.57 is remarkably similar to that on the training set (Chart 5). This robust performance gave us the confidence that the scoring function devised most likely has interaction terms and the formulation that are transferable and reliable enough to use for scoring protein–ligand complexes outside the training set. Contour scoring function performance is among the best scoring functions in the literature displaying good scoring power (Table 6). This ability to score protein–ligand complexes not in the training set, has allowed us to apply it to successfully design inhibitors for renin, 11β HSD-1 enzyme, LXR agonists, and BACE1 inhibitors [48,53–59].

The worst predicted activity for the complexes from pdb codes 2i0d and 1e5a are off by ~5 log units. The examination of the structure from 1e5a reveals that the compound bromophenol bound to the human transthyretin has the phenolic hydroxyl hydrogen bonded with the lysines from the two monomers, and the rest of the molecule interacting with non-polar residues (Fig. 2). The presence of two bromine atoms adjacent to the hydroxyl group would be treated as partially screened interaction with lysines, and the bromines treated as non-polar atoms may not electrostatically contribute with the Contour scoring function. The structure from 2i0d contains a large ligand with most of the multiple polar groups interacting poorly with the protein. It appears that in this case Contour assigned a large desolvation penalty for these polar groups.

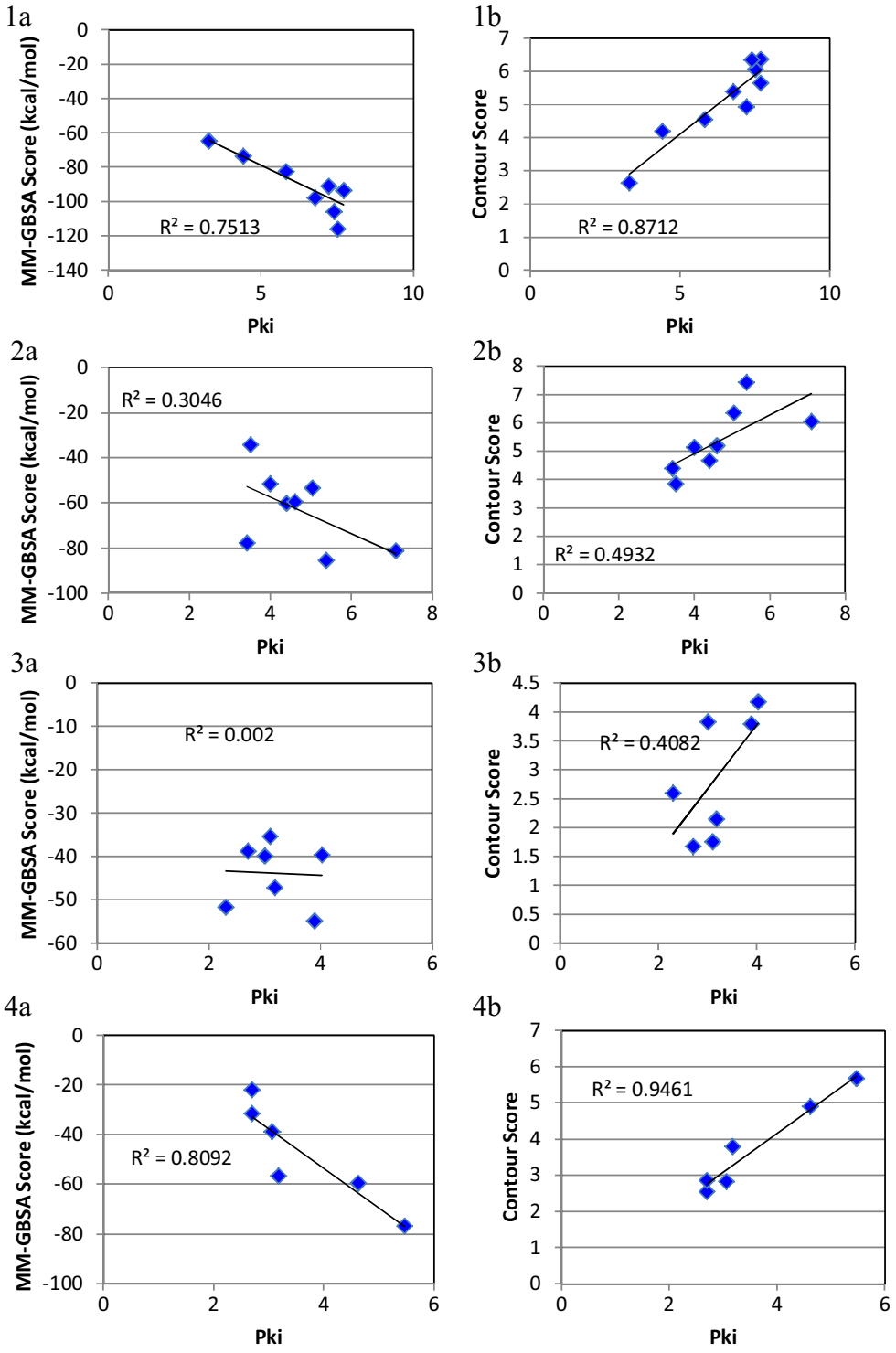

Chart 7. Comparison of the activity predictions by MM-GBSA and Contour scoring function for 4 congeneric series of BACE-1 inhibitors. Conformations of the BACE1 inhibitors were taken from the crystal structures and then superimposed into the protein conformation from 2OHU crystal structure. Both MM-GBSA and Contour obtained high correlations with R^2 greater than 0.7 for two series, and in addition, Contour achieved reasonable performance for the other 2 series.

Obviously these two cases support a need for an improved charging scheme.

3.5. Scoring and ranking power of Contour versus that of MM-GBSA

A reliable performance of the Contour scoring function beyond the training data set was further examined to validate the scoring power with a diverse set of crystal structures of BACE1 inhibitor complexes, and a more challenging test with a congeneric series of BACE1 inhibitors without crystal structures. BACE1 complex crystal structures with a broad range of activity (mM–nM), as demonstrated with the training set, provided a very good chance for the Contour scoring function to perform well. As expected a 0.55 correlation was obtained with BACE1 inhibitor complexes (Chart 6). As a comparator we used the OPLS force field based

Table 6
Comparison of Contour scoring function performance versus other scoring functions [35].

Scoring function	Correlation R	Correlation R^2	95% confidence interval
Contour	0.75	0.57	0.25
DS::Jain	0.40	0.16	0.34
DS:LigScore2	0.54	0.29	0.32
DS::LUDI3	0.50	0.25	0.32
DS::PLP1	0.66	0.44	0.28
DS::PMF	0.62	0.38	0.29
Drugscore^{CSD}::PairSurf	0.69	0.49	0.27
GOLD::ASP	0.59	0.35	0.30
GOLD::ChemScore	0.41	0.17	0.34
GOLD::GoldScore	0.15	0.02	0.37
GlideScore::XP	0.07	0.005	0.37
SYBYL::ChemScore	0.58	0.34	0.30
X-Score1.2::HMScore	0.73	0.53	0.26

MM-GBSA protocol from the Prime program to score these BACE1 crystal structures [60]. This protocol yielded a better performance with a correlation of 0.66, however qualitatively similar to that of Contour's performance (Chart 6). After comparing the structural similarity and binding poses of the ligands, four congeneric subsets of BACE1 crystal structures were created. These subsets were used for a detailed head-to-head comparison of the performances of Contour and MM-GBSA. Both MM-GBSA and Contour obtained high correlations with R^2 great than 0.7 for two series, and in addition, Contour achieved reasonable performance for the other 2 subsets (Chart 7). It is encouraging that Contour shows a robust performance close to the best MM-GBSA protocol available from Maestro [52]. This data is provided in the Supplementary Table S3.

4. Discussion

A novel zone based interaction model, representing the hybrid molecular orbitals, allowed us to capture a qualitative physical model that is sensitive to electronic environment of atoms. This model is capable of qualitatively representing the atoms and their interaction effects relevant for protein:ligand complexes. An advantage of this physical model is its ability to capture interatomic interactions that are sensitive to the hybridization state of the atoms involved, which is not possible with a conventional hard sphere model of atoms.

The explicit lone pair representation allows us to capture the directional interaction of hydrogen bonds much more accurately than those without them. The formal charges assigned for the hydrogen bond donor and the lone pairs are simple, but not consistent with quantum mechanical calculations. So a more reasonable representation of the charges for these moieties should be based on a suitable choice of a quantum mechanical method to partition these charges rationally to represent the zone polarity appropriately.

In the current model, halogens, F, Cl, Br, and I, are given zero charge with no positive interaction benefit in protein–ligand affinity calculation. However, their only contribution comes from desolvation.

The contact model used here accounts for interactions up to 5 Å, and the interactions beyond this distance are assumed to be screened. This assumption may be a good approximation in aqueous medium with high dielectric, but in the protein environment where long-range interactions could play a significant role in the binding affinity of ligands this could pose a challenge.

Despite the above limitations mentioned above the features represented by the Contour scoring function are able to capture key elements of binding interactions as demonstrated by its performance on the training set and the validation examples presented in this account. The scoring power of Contour is among the best as judged by its performance on the validation set from Wang's lab (Table 6) [35]. This ability is key to the success of our scoring function in identifying compounds designed by Contour's growth algorithm that have the likelihood of exhibiting activity. A modification is needed to improve the ranking power for it to be more useful for lead optimization, which comprises the majority of the drug design efforts. A careful examination of the mispredictions, mostly on the weaker side of affinity, appears due to the simple electrostatic model adopted by the scoring function. For instance, electrostatic repulsion arising due to the misassignment of formal charge on the terminal oxygen atom of the carbamate group, and on certain ether oxygens, etc., for renin inhibitors lead to incorrect affinity predictions. Another source of error is the inappropriate conformational preferences assigned due to lack of proper torsional parameters.

5. Conclusion

Contour scoring function consists of a unique physical model with electronic zones consistent with hybridization states of atoms. This model offers advantage over hard sphere models by providing a means to capture intermolecular interactions sensitive to direction and orientation of atoms. A simple electrostatic charge model adopted for the atomic zones predicts affinities of protein–ligand complexes consistently well across validation sets. Contour's binding affinity predictive power is comparable to the best scoring functions in the literature. The examination of mispredicted activities points to a need for an improved charge model in future development.

Acknowledgments

We thank Jun Shimada, Alexei Ischenko, David Lawson, Yuajie Ye, Jean-Pierre Wery, Zhongren Wu, Brian Mckeever, Kristi Fan, Yajun Zheng, Colin Tice, Larry Dillard, Yuri Bukthiyarov, Richard Harrison, and Jerry McGeehan for their help. We acknowledge valuable discussions with William Jorgensen of Yale University and Eugene Shakhnovich of Harvard University. We are grateful to Renxiao Wang of Shangai Institute of Organic Chemistry for providing us with the PDBbind validation set and the full set of scores.

Appendix A. Supplementary data

Supplementary data associated with this article can be found, in the online version, at http://dx.doi.org/10.1016/j.jmgm.2014.07.010.

References

[1] A. Fersht, Enzyme Structure and Mechanism, 2nd ed., W.H. Freeman and Company, New York, 1985, pp. 475.
[2] H. Gohlke (Ed.), Protein–Ligand Interactions, vol. 53, Wiley-VCH Verlag GmbH & Co. KGaA, Weinheim, 2012, pp. 1–339.
[3] H.X. Zhou, M.K. Gilson, Theory of free energy and entropy in noncovalent binding, Chem. Rev. 109 (9) (2009) 4092–4107.
[4] K.W. Harpole, K.A. Sharp, Calculation of configurational entropy with a Boltzmann-quasiharmonic model: the origin of high-affinity protein–ligand binding, J. Phys. Chem. B 115 (30) (2011) 9461–9472.
[5] M.J. Stone, NMR relaxation studies of the role of conformational entropy in protein stability and ligand binding, Acc. Chem. Res. 34 (5) (2001) 379–388.
[6] R.O. Dror, R.M. Dirks, J.P. Grossman, H. Xu, D.E. Shaw, Biomolecular simulation: a computational microscope for molecular biology, Annu. Rev. Biophys. 41 (2012) 429–452.
[7] P. Kollman, Free energy calculations: applications to chemical and biochemical phenomena, Chem. Rev. 93 (7) (1993) 2395–2417.
[8] W.L. Jorgensen, Efficient drug lead discovery and optimization, Acc. Chem. Res. 42 (6) (2009) 724–733.

[9] J.D. Chodera, D.L. Mobley, M.R. Shirts, R.W. Dixon, K. Branson, V.S. Pande, Alchemical free energy methods for drug discovery: progress and challenges, Curr. Opin. Struct. Biol. 21 (2) (2011) 150–160.
[10] H.J. Bohm, The development of a simple empirical scoring function to estimate the binding constant for a protein–ligand complex of known three-dimensional structure, J. Comput. Aided Mol. Des. 8 (3) (1994) 243–256.
[11] D.K. Gehlhaar, G.M. Verkhivker, P.A. Rejto, C.J. Sherman, D.B. Fogel, L.J. Fogel, S.T. Freer, Molecular recognition of the inhibitor AG-1343 by HIV-1 protease: conformationally flexible docking by evolutionary programming, Chem. Biol. 2 (5) (1995) 317–324.
[12] G. Jones, P. Willett, R.C. Glen, Molecular recognition of receptor sites using a genetic algorithm with a description of desolvation, J. Mol. Biol. 245 (1) (1995) 43–53.
[13] A.N. Jain, Scoring noncovalent protein–ligand interactions: a continuous differentiable function tuned to compute binding affinities, J. Comput. Aided Mol. Des. 10 (5) (1996) 427–440.
[14] M.D. Eldridge, C.W. Murray, T.R. Auton, G.V. Paolini, R.P. Mee, Empirical scoring functions: I. The development of a fast empirical scoring function to estimate the binding affinity of ligands in receptor complexes, J. Comput. Aided Mol. Des. 11 (5) (1997) 425–445.
[15] G. Jones, P. Willett, R.C. Glen, A.R. Leach, R. Taylor, Development and validation of a genetic algorithm for flexible docking, J. Mol. Biol. 267 (3) (1997) 727–748.
[16] H.J. Bohm, Prediction of binding constants of protein ligands: a fast method for the prioritization of hits obtained from de novo design or 3D database search programs, J. Comput. Aided Mol. Des. 12 (4) (1998) 309–323.
[17] G.M. Morris, D.S. Goodsell, R.S. Halliday, R. Huey, W.E. Hart, R.K. Belew, A.J. Olson, Automated docking using a Lamarckian genetic algorithm and an empirical binding free energy function, J. Comput. Chem. 19 (14) (1998) 1639–1662.
[18] I. Muegge, Y.C. Martin, A general and fast scoring function for protein–ligand interactions: a simplified potential approach, J. Med. Chem. 42 (5) (1999) 791–804.
[19] H. Gohlke, M. Hendlich, G. Klebe, Knowledge-based scoring function to predict protein–ligand interactions, J. Mol. Biol. 295 (2) (2000) 337–356.
[20] T.J. Ewing, S. Makino, A.G. Skillman, I.D. Kuntz, DOCK 4.0: search strategies for automated molecular docking of flexible molecule databases, J. Comput. Aided Mol. Des. 15 (5) (2001) 411–428.
[21] R. Wang, L. Lai, S. Wang, Further development and validation of empirical scoring functions for structure-based binding affinity prediction, J. Comput. Aided Mol. Des. 16 (1) (2002) 11–26.
[22] B.A. Grzybowski, A.V. Ishchenko, J. Shimada, E.I. Shakhnovich, From knowledge-based potentials to combinatorial lead design in silico, Acc. Chem. Res. 35 (5) (2002) 261–269.
[23] R.A. Friesner, J.L. Banks, R.B. Murphy, T.A. Halgren, J.J. Klicic, D.T. Mainz, M.P. Repasky, E.H. Knoll, M. Shelley, J.K. Perry, D.E. Shaw, P. Francis, P.S. Shenkin, Glide: a new approach for rapid, accurate docking and scoring. 1. Method and assessment of docking accuracy, J. Med. Chem. 47 (7) (2004) 1739–1749.
[24] C. Zhang, S. Liu, Q. Zhu, Y. Zhou, A knowledge-based energy function for protein–ligand, protein–protein, and protein–DNA complexes, J. Med. Chem. 48 (7) (2005) 2325–2335.
[25] H.F. Velec, H. Gohlke, G. Klebe, DrugScore(CSD)-knowledge-based scoring function derived from small molecule crystal data with superior recognition rate of near-native ligand poses and better affinity prediction, J. Med. Chem. 48 (20) (2005) 6296–6303.
[26] W.T. Mooij, M.L. Verdonk, General and targeted statistical potentials for protein–ligand interactions, Proteins: Struct. Funct. Bioinf. 61 (2) (2005) 272–287.
[27] A. Krammer, P.D. Kirchhoff, X. Jiang, C.M. Venkatachalam, M. Waldman, LigScore: a novel scoring function for predicting binding affinities, J. Mol. Graphics Modell. 23 (5) (2005) 395–407.
[28] S.Y. Huang, X. Zou, An iterative knowledge-based scoring function to predict protein–ligand interactions: I. Derivation of interaction potentials, J. Comput. Chem. 27 (15) (2006) 1866–1875.
[29] I. Muegge, PMF scoring revisited, J. Med. Chem. 49 (20) (2006) 5895–5902.
[30] P. Pfeffer, H. Gohlke, DrugScoreRNA—knowledge-based scoring function to predict RNA–ligand interactions, J. Chem. Inf. Model. 47 (5) (2007) 1868–1876.
[31] C.A. Sotriffer, P. Sanschagrin, H. Matter, G. Klebe, SFCscore: scoring functions for affinity prediction of protein–ligand complexes, Proteins: Struct. Funct. Bioinf. 73 (2) (2008) 395–419.
[32] S. Raub, A. Steffen, A. Kamper, C.M. Marian, AIScore chemically diverse empirical scoring function employing quantum chemical binding energies of hydrogen-bonded complexes, J. Chem. Inf. Model. 48 (7) (2008) 1492–1510.
[33] I. Reulecke, G. Lange, J. Albrecht, R. Klein, M. Rarey, Towards an integrated description of hydrogen bonding and dehydration: decreasing false positives in virtual screening with the HYDE scoring function, ChemMedChem 3 (2008) 885–897 (1870-7187 (electronic)).
[34] O.V. Stroganov, F.N. Novikov, V.S. Stroylov, V. Kulkov, G.G. Chilov, Lead finder: an approach to improve accuracy of protein–ligand docking, binding energy estimation, and virtual screening, J. Chem. Inf. Model. 48 (12) (2008) 2371–2385.
[35] T. Cheng, X. Li, Y. Li, Z. Liu, R. Wang, Comparative assessment of scoring functions on a diverse test set, J. Chem. Inf. Model. 49 (4) (2009) 1079–1093.
[36] S.Y. Huang, X. Zou, Inclusion of solvation and entropy in the knowledge-based scoring function for protein–ligand interactions, J. Chem. Inf. Model. 50 (2) (2010) 262–273.
[37] M. Xue, M. Zheng, B. Xiong, Y. Li, H. Jiang, J. Shen, Knowledge-based scoring functions in drug design. 1. Developing a target-specific method for kinase–ligand interactions, J. Chem. Inf. Model. 50 (8) (2010) 1378–1386.
[38] G. Neudert, G. Klebe, DSX: a knowledge-based scoring function for the assessment of protein–ligand complexes, J. Chem. Inf. Model. 51 (10) (2011) 2731–2745.
[39] Y.T. Tang, G.R. Marshall, PHOENIX: a scoring function for affinity prediction derived using high-resolution crystal structures and calorimetry measurements, J. Chem. Inf. Model. 51 (2) (2011) 214–228.
[40] Q. Shen, B. Xiong, M. Zheng, X. Luo, C. Luo, X. Liu, Y. Du, J. Li, W. Zhu, J. Shen, H. Jiang, Knowledge-based scoring functions in drug design: 2. Can the knowledge base be enriched? J. Chem. Inf. Model. 51 (2) (2011) 386–397.
[41] Z. Zheng, K.M. Merz, Ligand Identification Scoring Algorithm (LISA), J. Chem. Inf. Model. 51 (6) (2011) 1296–1306.
[42] J.D. Durrant, J.A. McCammon, NNScore 2.0: a neural-network receptor–ligand scoring function, J. Chem. Inf. Model. 51 (11) (2011) 2897–2903.
[43] L. Li, B. Wang, S.O. Meroueh, Support vector regression scoring of receptor–ligand complexes for rank-ordering and virtual screening of chemical libraries, J. Chem. Inf. Model. 51 (9) (2011) 2132–2138.
[44] A. Hamza, N.-N. Wei, C.-G. Zhan, Ligand-based virtual screening approach using a new scoring function, J. Chem. Inf. Model 52 (4) (2012) 963–974.
[45] G.L. Warren, C.W. Andrews, A.-M. Capelli, B. Clarke, J. LaLonde, M.H. Lambert, M. Lindvall, N. Nevins, S.F. Semus, S. Senger, G. Tedesco, I.D. Wall, J.M. Woolven, C.E. Peishoff, M.S. Head, A critical assessment of docking programs and scoring functions, J. Med. Chem. 49 (20) (2006) 5912–5931.
[46] R.D. Smith, J.B. Dunbar, P.M.-U. Ung, E.X. Esposito, C.-Y. Yang, S. Wang, H.A. Carlson, CSAR benchmark exercise of 2010: combined evaluation across all submitted scoring functions, J. Chem. Inf. Model. 51 (9) (2011) 2115–2131.
[47] S.A. Hayik, R. Dunbrack, K.M. Merz, Mixed quantum mechanics/molecular mechanics scoring function to predict protein–ligand binding affinity, J. Chem. Theory Comput. 6 (10) (2010) 3079–3091.
[48] A. Ishchenko, Z. Liu, P. Lindblom, G. Wu, K.-C. Jim, R.D. Gregg, D.A. Claremon, S.B. Singh, Structure-based design technology contour and its application to the design of renin inhibitors, J. Chem. Inf. Model. 52 (8) (2012) 2089–2097.
[49] F. Allen, The Cambridge structural database: a quarter of a million crystal structures and rising, Acta Crystallogr. Sect. B: Struct. Sci. 58 (3 Part 1) (2002) 380–388.
[50] R. Wang, X. Fang, Y. Lu, S. Wang, The PDBbind database: collection of binding affinities for protein–ligand complexes with known three-dimensional structures, J. Med. Chem. 47 (12) (2004) 2977–2980.
[51] Schrödinger Suite 2006 Protein Preparation Wizard, Schrödinger, LLC, New York, NY.
[52] Schrödinger Maestro Graphical User Interface, Maestro Version 2006, Schrödinger, LLC, New York, NY.
[53] Z. Liu, P. Lindblom, D.A. Claremon, S.B. Singh, Structure-based design technology CONTOUR and its application to drug discovery Innovations in Biomolecular Modeling and Simulations, vol. 2, The Royal Society of Chemistry, Cambridge, 2012, pp. 265–280 (Chapter 11).
[54] Z. Xu, S. Cacatian, J. Yuan, R.D. Simpson, L. Jia, W. Zhao, C.M. Tice, P.T. Flaherty, J. Guo, A. Ishchenko, S.B. Singh, Z. Wu, B.M. McKeever, B.B. Scott, Y. Bukhtiyarov, J. Berbaum, J. Mason, R. Panemangalore, M.G. Cappiello, R. Bentley, C.P. Doe, R.K. Harrison, G.M. McGeehan, L.W. Dillard, J.J. Baldwin, D.A. Claremon, Optimization of orally bioavailable alkyl amine renin inhibitors, Bioorg. Med. Chem. Lett. 20 (2) (2009) 694–699.
[55] C.M. Tice, Z. Xu, J. Yuan, R.D. Simpson, S.T. Cacatian, P.T. Flaherty, W. Zhao, J. Guo, A. Ishchenko, S.B. Singh, Z. Wu, B.B. Scott, Y. Bukhtiyarov, J. Berbaum, J. Mason, R. Panemangalore, M.G. Cappiello, D. Muller, R.K. Harrison, G.M. McGeehan, L.W. Dillard, J.J. Baldwin, D.A. Claremon, Design and optimization of renin inhibitors: orally bioavailable alkyl amines, Bioorg. Med. Chem. Lett. 19 (13) (2009) 3541–3545.
[56] C.M. Tice, W. Zhao, P.M. Krosky, B.A. Kruk, J. Berbaum, J.A. Johnson, Y. Bukhtiyarov, R. Panemangalore, B.B. Scott, Y. Zhao, J.G. Bruno, L. Howard, J. Togias, Y.J. Ye, S.B. Singh, B.M. McKeever, P.R. Lindblom, J. Guo, R. Guo, H. Nar, A. Schuler-Metz, R.E. Gregg, K. Leftheris, R.K. Harrison, G.M. McGeehan, L. Zhuang, D.A. Claremon, Discovery and optimization of adamantyl carbamate inhibitors of 11beta-HSD1, Bioorg. Med. Chem. Lett. 20 (22) (2010) 6725–6729.
[57] Z. Xu, C.M. Tice, W. Zhao, S. Cacatian, Y.J. Ye, S.B. Singh, P. Lindblom, B.M. McKeever, P.M. Krosky, B.A. Kruk, J. Berbaum, R.K. Harrison, J.A. Johnson, Y. Bukhtiyarov, R. Panemangalore, B.B. Scott, Y. Zhao, J.G. Bruno, J. Togias, J. Guo, R. Guo, P.J. Carroll, G.M. McGeehan, L. Zhuang, W. He, D.A. Claremon, Structure-based design and synthesis of 1,3-oxazinan-2-one inhibitors of 11beta-hydroxysteroid dehydrogenase type 1, J. Med. Chem. 54 (17) (2011) 6050–6062.
[58] L. Jia, R.D. Simpson, J. Yuan, Z. Xu, W. Zhao, S. Cacatian, C.M. Tice, J. Guo, A. Ishchenko, S.B. Singh, Z. Wu, B.M. McKeever, Y. Bukhtiyarov, J.A. Johnson, C.P. Doe, R.K. Harrison, G.M. McGeehan, L.W. Dillard, J.J. Baldwin, D.A. Claremon, Discovery of VTP-27999, an alkyl amine renin inhibitor with potential for clinical utility, ACS Med. Chem. Lett. 2 (10) (2011) 747–751.
[59] J. Yuan, R.D. Simpson, W. Zhao, C.M. Tice, Z. Xu, S. Cacatian, L. Jia, P.T. Flaherty, J. Guo, A. Ishchenko, Z. Wu, B.M. McKeever, B.B. Scott, Y. Bukhtiyarov,

J. Berbaum, R. Panemangalore, R. Bentley, C.P. Doe, R.K. Harrison, G.M. McGeehan, S.B. Singh, L.W. Dillard, J.J. Baldwin, D.A. Claremon, Biphenyl/diphenyl ether renin inhibitors: filling the S1 pocket of renin via the S3 pocket, Bioorg. Med. Chem. Lett. 21 (16) (2011) 4836–4843.
[60] Prime Version 3.1, Schrödinger, LLC, New York, NY, 2012.
[61] M. Congreve, D. Aharony, J. Albert, O. Callaghan, J. Campbell, R.A. Carr, G. Chessari, S. Cowan, P.D. Edwards, M. Frederickson, R. McMenamin, C.W. Murray, S. Patel, N. Wallis, Application of fragment screening by X-ray crystallography to the discovery of aminopyridines as inhibitors of beta-secretase, J. Med. Chem. 50 (6) (2007) 1124–1132.
[62] Discovery Studio, Discovery Studio Version 3.5.0.12158, Accelrys, Inc., San Diego, CA, 2012.
[63] W.D. Cornell, P. Cieplak, C.I. Bayly, I.R. Gould, K.M. Merz Jr., D.M. Ferguson, D.C. Spellmeyer, T. Fox, J.W. Caldwell, P.A. Kollman, A second generation force field for the simulation of proteins, nucleic acids, and organic molecules, J. Am. Chem. Soc. 117 (1995) 5179–5197.